Thermal effects on electron-phonon interaction in silicon nanostructures

Rajesh Kumar,* Vivek Kumar, and A. K. Shukla†

Department of Physics, Indian Institute of Technology Delhi, New Delhi 110016, India

(Dated: December 15, 2009)

Abstract

Raman spectra from silicon nanostructures, recorded using excitation laser power density of 1.0 kW/cm^2 , is employed here to reveal the dominance of thermal effects at temperatures higher than the room temperature. Room temperature Raman spectrum shows only phonon confinement and Fano effects. Raman spectra recorded at higher temperatures show increase in FWHM and decrease in asymmetry ratio with respect to its room temperature counterpart. Experimental Raman scattering data are analyzed successfully using theoretical Raman line-shape generated by incorporating the temperature dependence of phonon dispersion relation. Experimental and theoretical temperature dependent Raman spectra are in good agreement. Although quantum confinement and Fano effects persists, heating effects start dominating at higher temperatures than room tempaerature.

PACS numbers: 78.67.f; 63.22.-m; 78.30.j

Keywords: Phonon confinement, Fano interaction, Raman spectra, Silicon nanostructures

Raman scattering from all forms of solids (single crystal, poly-and nanocrystalline) gives many information about its vibrational properties and the crystallanity. Quantum confinement effect in semiconductor nanostructures(NSs) can also be investigated very effectively by Raman spectroscopy by close analysis of the Raman line-shape. A symmetric Raman spectrum with very narrow line width is observed from crystalline materials as a signature of zone center optic phonon mode having Lorentzian line-shape. Any deviation in Raman line-shape symmetry, frequency or line width could be due to various reasons associated with quantum confinement effect, heating effect, electron-phonon interactions or any combination of these. For silicon (Si), a 4 cm^{-1} broad symmetric Raman line-shape centered at 520.5 cm^{-1} is observed at room temperature. Temperature dependence of Raman line-shape from crystalline Si (c-Si) has been studied by many authors[1,2,3,4]. The Lorentzian Raman line-shape from c-Si becomes wider and shifts to lower wavenumber side at elevated temperature[3]. As a result of increase in the temperature the stokes and antistokes intensity ratio also decreases, which in turn is used to calculate the sample temperature[4,5]. Asymmetric Raman line-shapes are observed from heavily doped Si due to Fano interaction[6]. Fano interaction takes place as a consequence of interference between discrete phonons and continuum of electronic states (available as a consequence of heavy doping) in heavily doped Si[7,8]. Asymmetric Raman line-shapes can also be observed from nanostructures (NSs)[9,10,11]. In Si NSs, the phonons are confined within the small NSs causing the breakdown of $\overrightarrow{k} = 0$ Raman selection rule and all optic phonons take part in the Raman scattering[12,13]. As a result Raman line-shape becomes asymmetric and downshifted for Si NSs.

Attempts have been taken to investigate a combination of different effects that may change Raman line-shape. Recently, a combined effect of photo-excited Fano interaction and phonon confinement is also reported for Si NSs[14,15]. Temperature dependent Raman scattering studies for Si NSs for temperatures above 300 K have been reported previously[16,17,18,19,20,21] by combining heating and confinement effects. Many authors[17,18,19,20,21] explain the Raman line-shape at elevated temperature by simply considering the temperature dependence of Raman peak position and FWHM as formulated by Balkanski et al[4]. He used the higher order anharmonicity in light scattering by optical phonons to incorporate the effect of temperature on zone center optic phonons only. Narsimhan and Vanderbilt[22] have studied the phonon-phonon interaction in Si to calculate the contribution from anharmonicity to phonon lifetime and frequency shifts. They have shown that Γ and L point optic phonons

show different temperature dependence from each other. This means that not only the zone center phonons but the whole phonon dispersion relation change as a function of temperature. Thus, one may expect that temperature dependence of Raman line-shape from Si NSs (where all phonons participate in the Raman scattering) should be calculated by considering the temperature dependence of whole phonon dispersion relation and not by simple considering the peak shift. Same consideration should be taken care of when there is a possibility of Fano interaction as well.

In this Report, we present temperature dependence of photo-excited Fano interaction in Si NSs prepared by laser induced etching (LIE) technique[23]. Raman spectra are recorded using excitation laser power density of 1.0 kW/cm^2 at four sample temperatures in the range 300 K - 600 K. Room temperature Raman spectra for excitation laser power density of 1.0 kW/cm^2 shows a combined effect of phonon confinement and photo-excited Fano interaction. Experimental Raman spectra recorded at higher temperature show effect of temperature as well in terms of changes in the Raman line-shape. Temperature dependent changes in Raman line-shape have been explained theoretically by considering the temperature dependence of whole phonon dispersion relation as suggested by Narsimhan and Vanderbilt[22]

The Si NSs sample under investigation is fabricated by the LIE technique[23]. The LIE is done by immersing a Si wafer 48% HF acid and then focusing a 500 mW argon-ion laser beam (E_{ex} = 2.41 eV) for 45 minutes. Raman scattering was excited using photon energy 2.41 eV of the argon-ion laser with laser power density of 1.0 kW/cm^2 . The reason for choosing low laser power density is to avoid heating of the sample during Raman recording. Sample was heated using the heating arrangement on the sample holder to study the temperature dependent Raman scattering. Raman spectra were recorded by employing a SPEX-1403 doublemonochromator with HAMAMATSU (R943-2) photomultiplier tube arrangement and an argon ion laser (COHERENT, INNOVA 90).

Figure 1 shows the high resolution atomic force microscope (AFM) image of the Si NSs prepared by LIE technique. The shown AFM image is taken from the inside of the pore walls in the sample[24]. The AFM image shows the formation of Si NSs having sizes in the range of a few nanometers with very narrow size distribution. Quantum confinement is expected within these Si NSs because the sizes are comparable to the Bohr exciton radius (5 nm) of Si[25]. Raman experiments are done to investigate any possibility of phonon confinement effect in Si NSs. Figure 2(a) shows the room temperature Raman spectrum from Si NSs recorded

using excitation laser power density of 1 kW/cm^2 . The asymmetric Raman spectrum in Fig. 2(a) is red-shifted and broader in comparison to its c-Si counterpart. Asymmetrical broadening and red-shift is attributed to a combined effect of quantum confinement and photo-excited Fano interaction[13,14]. The Fano interaction takes place between the discrete phonon Raman scattering and quasi-continuum electronic Raman scattering[26]. Presence of quasi-continuum of electronic states available for electronic Raman scattering have been investigated using photoluminescence spectroscopy in our previous reports[26].

To see the effect of heating on Fano interaction, Raman spectra from the Si NSs have been recorded at different temperatures using excitation laser power density of 1.0 kW/cm^2 as displayed in Figs. 2(b) - 2(d). Sample temperature is estimated from the stokes and antistokes Raman intensity ratio[4,5]. Raman spectra at higher temperatures in Figs. 2(b) - 2(d) reveal that the red-shift and FWHM increase with increasing sample temperature. We attribute the changes in Raman features to a combined effect of quantum confinement effect, Photo-excited Fano interaction and heating effect. To theoretically fit the experimentally observed Raman data in Fig. 2, we have modified the Raman line-shape from Si NSs by including the temperature dependence of phonon dispersion relation. The modified temperature dependent Raman line-shape from Si NSs can be written as follows to incorporate the temperature dependent Fano interaction:

$$I(\omega,T) \propto \int_{L_1}^{L_2} N(L) \left[\int_0^1 \left\{ \frac{(\varepsilon+q)^2}{1+\varepsilon^2} \right\} e^{\frac{-k^2L^2}{4a^2}} d^2k \right] dL \qquad (1)$$

where, $\varepsilon = \frac{\omega-\omega(k,T)}{\gamma/2}$ and 'q' is Fano asymmetry parameter. The 'k' is the phonon wave vector. The γ, L and 'a' are the line width, crystallite size and lattice constant respectively. The '$N(L)$' is a Gaussian function of the form $N(L) \cong e^{-\left\{\frac{L-L_0}{\sigma}\right\}^2}$ included to account for the size distribution of the Si NSs. The L_0, σ, L_1 and L_2 are the mean crystallite size, the standard deviation of the size distribution, the minimum and the maximum confinement dimensions respectively. The $\omega(k,T)$ is the temperature dependent phonon dispersion relation of the optic phonons of c-Si given by $\omega(k,T) = \sqrt{A(T) + B(T)cos\left(\frac{\pi k}{2}\right)}$. Temperature dependent parameters, $A(T)$ and $B(T)$ have been taken from the analysis done by Narsimhan and Vanderbilt[22]. They have calculated the downshift in 'Γ' and 'L' point optic phonons as a function of temperature. Thus, the value of 'Γ' and 'L' point phonon frequency can be known at a given temperature. The 'L' point phonon frequency is utilized to find the value of A by using $k = 1$ in the phonon dispersion relation written above and B can be calculated by

utilizing 'Γ' point ($k = 0$) phonon frequency value. The values of $A(T)$ and $B(T)$, calculated in this way for Raman fitting, are summarized in Table I. At room temperature (300 K), the Eq. (1) reduces to the Raman line-shape having only quantum confinement effect and photo-excited Fano interaction as used in our earlier papers[14,15]. The room temperature Raman data in Fig. 2(a) is best fitted for fitting parameters L_0, L_1, L_2 and σ of 4 nm, 3 nm, 5 nm and 2 nm respectively. Another fitting parameter in Eq.(1) is Fano asymmetry parameter 'q'. The value of $|q| = 11$ is obtained by fitting experimental data in Fig. 2(a) with Eq. (1). The value of 'q' was kept constant while fitting the Raman spectra in Figs. 2(b)-2(d) because thermally generated carriers could be treated to be negligible for Fano interaction. Theoretically fitted Raman line-shapes generated using Eq. (1) are shown by continuous lines in Fig. 2. It is evident from theoretical Raman fitting of experimental Raman data that room temperature Raman scattering has contribution only from phonon confinement effect and photo-excited Fano interaction. Raman spectra at higher temperatures have additional contribution from heating effect in addition to the phonon confinement and Fano effects. As a result of heating, the FWHM and phonon softening increases in Fig. 2 but asymmetry ratio (asymmetry ratio is defined as $\frac{\gamma_l}{\gamma_h}$, where γ_l and γ_h are the half widths on the lower and higher side of the Raman peak position) decreases. Asymmetry ratios and FWHMs of Raman line-shapes in Fig. 2 are compared in Fig. 3. When sample temperature is increased, Raman half widths increase equally on both the sides of the peak position. As a result, asymmetry ratio ($\frac{\gamma_l}{\gamma_h}$) decreases as heating effect dominates over the phonon confinement and Fano effects, which is fixed in our sample. In other words, phonon confinement and Fano effects are dominated by heating effects.

Temperature dependent experimental Raman data from Si NSs in Fig. 2 show a good theoretical fitting using Eq. (1). This means that the temperature dependence of Raman scattering should be incorporated in theoretical Raman line-shape by considering the temperature dependence of the whole phonon dispersion relation as done in our case. This type of analysis is necessary because the thermal effect is different for Γ and L point phonons as reported by Narsimhan and Vanderbilt[22]. As a result, Γ and L points on optic branch downshift by different amounts at higher temperatures. This fact could be taken into account only by taking the temperature dependence of whole phonon dispersion relation. This analysis will be extremely important in understanding any non-linear Fano interaction in nanoscale materials[27].

In summary, temperature related effects are found to dominate over the phonon confinement and Fano interaction in Si NSs in Raman spectra recorded at higher temperatures than room temperature. The room temperature Raman spectrum recorded using laser power density of 1 kW/cm^2 show contributions from photo-excited Fano interaction and phonon confinement effect. Increase in FWHM and decrease in asymmetry ratio in Raman line-shape were observed as a result of increasing temperature. Theoretical analyses of Raman spectra are done by fitting the experimental Raman data with theoretical Raman line-shape obtained by appropriately considering the phonon confinement effect and Fano interaction. Temperature dependence is incorporated in theoretical Raman line-shapes by considering the temperature dependence of whole phonon dispersion relation. Temperature dependent phonon dispersion relation is obtained by considering different downshifts in Γ and L point phonons in phonon dispersion curve at a given temperature. A good agreement between experimental and theoretical Raman results reveals that it is more appropriate to incorporate temperature dependence of full phonon dispersion relation to explain the temperature dependent Raman spectra from Si NSs.

Authors are thankful to Prof. V.D. Vankar for many useful discussions. Authors acknowledge the financial support from the Department of Science and Technology, Govt. of India under the project "Linear and nonlinear optical properties of semiconductor/metal nanoparticles for optical/electronic devices". One of the authors (R.K.) acknowledges financial assistance from National Research Council (NRC). NINT is operated as a partnership between the NRC and the University of Alberta and is jointly funded by the Govt. of Canada, the Govt. of Alberta and University of Alberta. One of the authors (V.K.) acknowledges the financial support from University Grants Commission (UGC), India. Technical support from Mr. N.C. Nautiyal is also acknowledged.

---

* Electronic address: rajesh2@ualberta.ca; Present Address: National Institute for Nanotechnology (NINT), University of Alberta, Edmonton T6G 2M9, CANADA

† Electronic address: akshukla@physics.iitd.ernet.in

[1] T.R. Hart, R.L. Aggarwal B. Lax, Phys. Rev. B **1**, 638 (1970)

[2] R. Tsu, J.G. Hernandez, Appl. Phys. Lett. **41**, 1016 (1981)

[3] J. Raptis, E. Liarokapis, E. Anastassakis, Appl. Phys. Lett. **44**, 125 (1984)

[4] M.Balkanski, R.F. Wallis, E. Haro, Phys. Rev. B **28**, 1928 (1983).

[5] H.S.Mavi, S. Prusty, A.K. Shukla, S.C. Abbi, Thin Solid Films **425**, 90 (2003).

[6] U. Fano, Phys. Rev. **124**, 1866 (1961).

[7] M. Balkanski, K.P. Jain, R. Beserman, M. Jouanne, Phys. Rev. B **12**, 4328 (1975).

[8] M. Becker, U.Gosele, A. Hofmann and S. Christiansen, J.Appl. Phys. **106**, 074515 (2009).

[9] L. Sirleto, M.A. Ferrara, B. Jalali, I. Rendina, J. Opt. A: Pure and Appl. Opt. **8**, 8574 (2006).

[10] S.B. Concari, R.H. Buitrago, Semicond. Sci. Technol **18**, 864 (2003)

[11] H.S. Mavi, A.K. Shukla, R. Kumar, S. Rath, B. Joshi, S.S. Islam, Semicond. Sci. Technol **21**, 1627 (2006).

[12] H. Richter, Z.P. Wang, L. Ley, Solid State Commun. **39**, 625 (1981).

[13] I.H. Campbell, P.M. Fauchet, Solid State Commun. **58**, 739 (1986).

[14] R.Kumar, H.S. Mavi, A.K. Shukla, V.D. Vankar, J. Appl. Phys. **101**, 064315 (2007).

[15] R. Kumar, A.K. Shukla, H.S. Mavi, V.D. Vankar,Nanoscale Res. Lett. **3**, 105 (2008).

[16] P. Mishra, K.P. Jain, Phys. Rev. B **62**, 14790 (2000).

[17] G. Faraci, S.Gibilisco and A.R. Pennisi Rev. B **80**, 193410 (2009).

[18] J. Niu, J. Sha, D. Yang, Scripta Mater. **55**, 183 (2006).

[19] R. Jalilian, G.U. Sumanasekera, H. Chandrasekharan, M.K. Sunkara, Phys. Rev. B **74**, 155421 (2006).

[20] M.J. Konstantinovic, Physica E **38**, 109 (2007).

[21] K.W. Adu, H.R. Gutierrez, U.J. Kim, P.C. Eklund, Phys. Rev. B **73**, 155333 (2006).

[22] S. Narasimhan, D. Vanderbilt, Phys. Rev. B **43**, 4541 (1991).

[23] H.S. Mavi, B.G. Rasheed, A.K. Shukla, S.C. Abbi, K.P. Jain, J. Phys. D: Appl. Phys. **34**, 292 (2001).

[24] R. Kumar, H.S. Mavi, A.K. Shukla, Micron **39**, 287 (2008).

[25] A.G. Cullis, L.T. Canham, P.D.J. Calcott, J. Appl. Phys. **82**, 909 (1997).

[26] A.K. Shukla, R. Kumar and V. Kumar, J. Appl. Phys. **In Press**, (2009)

[27] M. Kroner, A.O. Govorov, S.Remi, B. Biedermann, S. Seidl, A. Badolato, P.M. Petroff, W. Zhang,R. Barbour, B.D. Gerardot, R.J. Warburton, K. Karrai, Nature **451**, 311 (2008)

Temperature (K)	A(cm^{-2})	B(cm^{-2})	$\gamma(cm^{-1})$
300	171400	100000	4.0
400	170417	99011.4	4.95
500	169223.6	98717.2	6.36
600	167819.77	98369.25	7.93

TABLE I: Temperature dependent parameters used in Eq.(1)

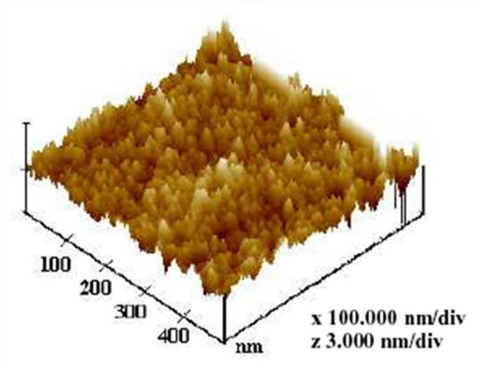

FIG. 1: (**Color online**) AFM image of silicon nanostructures prepared by laser induced etching method.

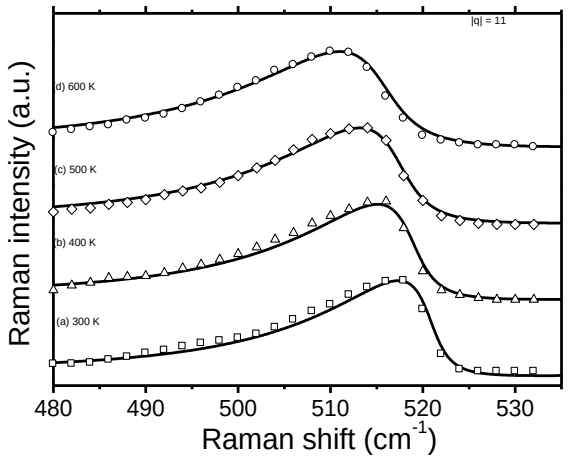

FIG. 2: Raman spectra from silicon nanostructures at different sample temperatures from 300 K to 600 K recorded at excitation laser power density of 1.0 kW/cm^2 . Discrete points are experimentally recorded data and continuous lines are theoretical fitting using Eq. (1) by considering the temperature effect on photo-excited Fano effect.

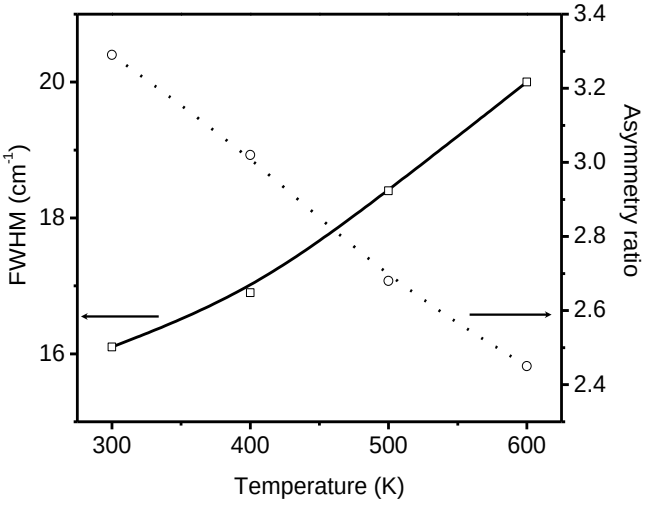

FIG. 3: Temperature dependent variation of asymmetry ratio and FWHM of Raman spectra from silicon nanostructures shown in Fig.2.